INTERNATIONAL JOURNAL OF
NUMERICAL ANALYSIS AND MODELING
Volume 18, Number 3, Pages 384–398

A STOCHASTIC GRADIENT DESCENT METHOD FOR THE DESIGN OF OPTIMAL RANDOM INTERFACE IN THIN-FILM SOLAR CELLS

DAN WANG[1], YANZHAO CAO[2], QIANG LI[3], AND JIHONG SHEN[4]

Abstract. Random rough texture design can be used to find the optimal design of random surfaces in thin film solar cells to increase their absorbing efficiency. We formulate the design problem as an optimal control problem under a PDE constraint. To lower the computational cost, the stochastic gradient method is employed to find the optimal surface. Numerical results show that the optimally obtained random texture has a much higher absorption rate in comparison with flat panels.

Key words. Optimal design, Helmholtz equation, transverse magnetic polarization, stochastic gradient decent method.

1. Introduction

Solar energy may be the cleanest renewable energy among all kinds of energy at present. With the traditional fossil fuel energy sources such as oil, coal, and gas running out, the energy crisis is aggravating. On the other hand, the solar energy can be used widely to meet the rapidly increasing energy demand [1].

Photovoltaics (often shortened as PV) is the conversion of solar light into electricity using semiconducting materials that exhibit the photovoltaic effect. A photovoltaic system converts the Sun's radiation, in the form of light, into usable electricity with the help of solar cell panels. Each of the solar cell panel contains a number of solar cells. There are mainly two types of solar cells: crystalline silicon and thin film solar cells.

Due to the high cost of crystalline silicon solar cells, the material purity and manufacturing process are limited. Compared to crystalline silicon solar cells, the lower cost of thin film solar cells undoubtedly provides favorable conditions for its development. A typical thin film solar cells are coated with p-i-n semiconductor film on the transparent conductive oxide film under the glass surface, and an electrode plate is plated on the back. Thin film solar cells consume fewer materials and only need tens of nanometers to hundreds of nanometers in thickness to achieve photoelectric conversion. However, the thin film solar cells have lower efficiency.

Since the first reports on practical microcrystalline cells in 1994, much research effort has been done worldwide into the development of both fundamental knowledge and technological skills that are needed to improve thin film silicon multi-junction solar cells. In addition, an efficient trapping structure can be designed to make amorphous silicon films absorb and utilize sunlight as much as possible. The absorption of more photons also provides a guarantee for improving the photoelectric conversion efficiency of thin film cells. There are many ways to increase the absorption efficiency of solar cells. The commonly used trapping techniques are: surface velvet, antireflection film, surface plasmon, reflector on the back of battery , and so on [2, 3, 4]. Another type of way to increase the efficiency is using randomly

Received by the editors December 22, 2020.
2000 *Mathematics Subject Classification.* 35, 65N30, 92.

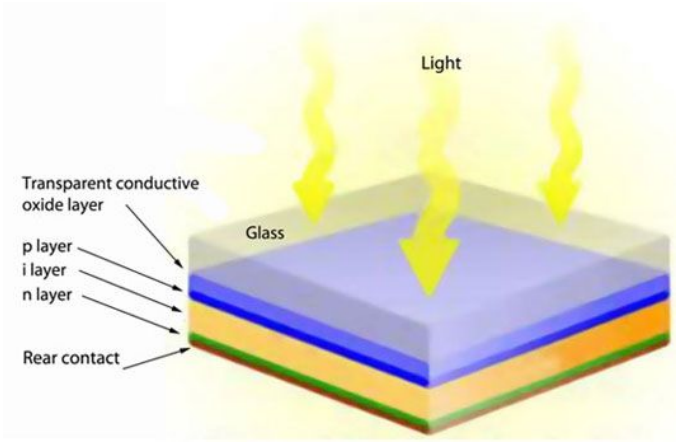

FIGURE 1. A typical structure of thin-film solar cells.

textured interface to trap the optical light [5, 6, 7, 8]. When the random interface is introduced into the contact surface of the solar cell, the light is reflected into the cell for many times to increase the optical path. In this way, the optical thickness of the thin film cell can be increased as much as possible without changing the physical thickness of the thin film cell. It is worth mentioning that by controlling the deposition parameters of TCO thin films sputtered on glass substrates, we can realize the fabrication of TCO surface layer can greatly improve the efficiency of thin film solar cells [9, 11]. The existing commercial solar cells have Asahi-U structure, Neuchatel structure and so on. Here we refer to some deterministic texture optimization design [10, 12], as well as the following deterministic shape optimization problems in physics and engineering. Most of the previous research on random texture optimization is based on certain ad hoc schemes. Mainly by calculating the absorption of several selected statistical parameters to select the parameter values that produce the maximum absorptivity. The optimal solution obtained in this way depends to a large extent on the selected set of statistical parameters. If the optimal parameters are not in the set, we will not be able to find the corresponding parameter values of the optimal solution.

There are two basic polarizations of light waves: transverse electric (TE) polarization and transverse magnetic (TM) polarization. These two kinds of polarization provide the basic for determining the light wave electric field and magnetic field at a certain position in the solar cell structure. The TE model was studied in [8]. In this paper, we focus on the transverse magnetic polarization. As in [8], we first reduce the modeling problem to an optimization problem with a PDE constraint. Unlike [8] where the gradient descent method was used to find the optimal interface minimizing the radiation, in this study, we use the stochastic gradient descent method (SGD) [13] for the same purpose. In the gradient descent method, the Monte-Carlo method is used to approximate the expectation of the cost function, which makes it extremely expensive when a large size of samples needs to be used to match the error of discretizing the Helmholtz equation. On the other hand, only one sample is used at each iteration for the SGD method. Our numerical experiment indicates that, with the same accuracy, the cost of the SGD method is only a tiny fraction of that for the gradient descent method.

The rest of the paper is arranged as follows. In Section 2, we introduce the mathematical model of the random rough surface problem. Section 3 focuses on the optimization design problem and describes the gradient calculation of the objective function. Several numerical experiments are presented in Section 4 to to demonstrate the efficiency of the stochastic gradient descent method and the optimal interface.

2. Mathematical models

2.1. Scattering problem. We aim to use a two-dimensional model through the theory of trapping structure in achieving the optimizing the efficiency of thin film solar cells. Because the index contrast between the glass substrate and TCO surface layer is not obvious, for simplicity, we do not explicitly consider the glass substrate. We assume that the battery is composed of two layers as shown in Figure 2: a transparent conducting oxide(TCO) layer on the top and an absorbing layer on the bottom. Our goal is to find the interface between the TCO layer and absorption layer which optimizes the collection rate of incident light by increasing the photon optical path. Here we assume that the bottom edge of the model is a perfect reflector; that is, there is no energy conversion on the bottom surface. For simplicity, we also assume that the structure is periodic with period Λ. The contact surface in the middle can be regarded as adding a random disturbance to the plane $y = a$. Let $(\Omega, \mathcal{F}, \mathbb{P})$ be a complete probability space. For each sample $\omega \in \Omega$, denote the interface as $\Gamma(\omega) := \{(x, y) \mid y = h(x) = a + f(\omega; x)\}$. We denote the TCO and absorption layer as

$$D_1(\omega) := \{(x, y) \mid x \in (0, \Lambda), 0 < y < h(\omega; x)\}$$

and

$$D_2(\omega) := \{(x, y) \mid x \in (0, \Lambda), h(\omega; x) < y < \infty\}$$

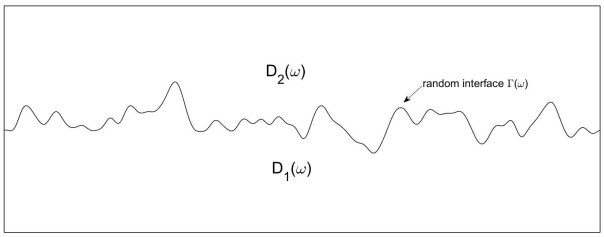

FIGURE 2. Scattering problem in the bounded domain D.

In this paper, we consider the magnetic field H under transverse magnetic polarization; that is, H is of the form of $(0, 0, u)$. Assume that the incident wave is the time harmonic plane wave $u^i = e^{-ik_0 qy}$, where k_0 is the free space wavenumber, and q is the refractive index of the TCO layer. The total field u after the scattering is composed of incident wave u^i and scattered wave u^s, i.e., $u = u^i + u^s$.

For any given sample ω, the total field u satisfies

$$\begin{cases} \nabla \cdot (\varepsilon_r^{-1} \nabla u(\omega; \cdot)) + k_0^2 u(\omega; \cdot) = 0 & \text{in } D_\Lambda \backslash \Gamma(\omega), \\ u(\omega; 0, y) = u(\omega; \Lambda, y), \\ \partial_\nu u(\omega; x, 0) = 0, \quad 0 < x < \Lambda, \end{cases} \tag{1}$$

where

$$\varepsilon_r = \begin{cases} \varepsilon_{r,1}, & y < h(\omega; x), \\ \varepsilon_{r,2}, & y > h(\omega; x). \end{cases}$$

Here ν is the outer normal vector, ε_r is the relative permittivity value, $\varepsilon_{r,1}$ and $\varepsilon_{r,2}$ are the relative permittivity value of the absorption layer and the TCO layer, respectively. The permittivity of the solar cell is $\varepsilon = \varepsilon_r \cdot \varepsilon_0$, where ε_0 is the permittivity value in the vacuum. In addition, we assume that the continuity conditions are satisfied along the interface:

$$u_+(\omega; x, h(\omega, x)) = u_-(\omega; x, h(\omega, x)), \tag{2}$$

$$\varepsilon_{r,2}^{-1}\partial_\nu u_+(\omega; x, h(\omega, x)) = \varepsilon_{r,1}^{-1}\partial_\nu u_-(\omega; x, h(\omega, x)). \tag{3}$$

To formulate the scattering optimization problem, we consider $y = b$ as an artificial upper boundary of the region, where $b > \max\limits_{0<x<\Lambda} h(\omega; x)$. We will apply the DtN mapping condition for the scattered field u^s given by

$$u^s(x, y) = \sum_{n\in Z} \widehat{u}_n^s(\omega; y)e^{i\alpha_n x}$$

where $\alpha_n = \frac{2\pi n}{\Lambda}$, $\widehat{u}_n^s(\omega, y) = \frac{1}{\Lambda}\int_0^\Lambda u^s(\omega; x, y)e^{-i\alpha_n x}dx$.

Denote $k = k_0\sqrt{\varepsilon_{r,2}}$. For a given sample ω , we have the expression of the scattering filed above the random interface $\Gamma(\omega)$ given by

$$u^s(\omega; \cdot) = \sum_{n\in Z} \widehat{u}_n^s(\omega; b)e^{i\alpha_n x + i\eta_n(y-b)},$$

where

$$\eta_n = \begin{cases} \sqrt{k_0^2\varepsilon_{r,2} - \alpha_n^2}, & k > \alpha_n, \\ i\sqrt{\alpha_n^2 - k_0^2\varepsilon_{r,2}}, & k < \alpha_n. \end{cases} \tag{4}$$

Then, on the upper boundary $y = b$,

$$\partial_y u^s(\omega; x, b) = \sum_{n\in Z} i\eta_n \widehat{u}_n^s(\omega; b)e^{\alpha_n} =: T[u^s(\omega; x, b)].$$

By direct calculation we have

$$\partial_y u(\omega; x, b) = T(u(\omega; x, b)) + g$$

where $g = -2ike^{-ikb}$. Therefore, for each sample ω, the scattering problem can be calculated in the bounded region D as,

$$\begin{cases} \nabla(\varepsilon_r^{-1}\nabla u(\omega; \cdot) + k_0^2 u(\omega; \cdot) = 0 & \text{in } D_\Lambda\backslash\Gamma(\omega), \\ u(\omega; 0, y) = u(\omega; \Lambda, y), & 0 < y < b, \\ \partial_\nu u(\omega; x, 0) = 0, & 0 < x < \Lambda, \\ \partial_y u(\omega; x, b) = T(u(\omega; x, b)) + g & 0 < x_1 < \Lambda. \end{cases} \tag{5}$$

2.2. Representation of random surfaces. Assume that the random texture surface $h = h(\omega; x)$ is a random perturbation of the reference surface $y = a$:

$$h(\omega; x) = a + f(\omega; x)$$

where $f = f(\omega; x)$ is a stationary Gaussian process whose mean value is 0, and the covariance function is

$$c(x_1 - x_2) = \sigma^2 exp(-\frac{|x_1 - x_2|^2}{l^2})$$

where σ is the surface root mean square(RMS) height and $0 < l \ll \Lambda$ is the correlation length. The random field f can be expanded using Karhunnen-Loéve expansion [14]. Since $f = f(\omega; x)$ is a periodic function with period Λ, we can perform Fourier expansion on the covariance equation $c = c(x)$. Noting that c is an even function, it follows that

$$c(x) = \sigma^2 \Big[\frac{\widehat{c_0}}{2} + \sum_{p=1}^{\infty} \widehat{c_p} cos(\frac{2p\pi x}{\Lambda}) \Big]$$

where $\widehat{c_0}$, $\widehat{c_1}$, $\widehat{c_2}$, $\cdots$ are the Fourier cosine expansion coefficients of the correlation function $\exp(-|x_1 - x_2|^2/l^2)$. For the covariance operator

$$K\varphi(x_1) := \int_0^d c(x_1 - x_2)\varphi(x_2)dx_2,$$

its eigenvalues are given by

$$\lambda_j = \frac{\sigma^2 \Lambda \widehat{c_j}}{2}, j = 0, 1, 2 \ldots,$$

and the corresponding eigenfunctions are

$$\varphi_j(x) = \begin{cases} \sqrt{\dfrac{1}{\Lambda}}, & j = 0, \\ \sqrt{\dfrac{2}{\Lambda}} \cos\left(\dfrac{2j\pi x}{\Lambda}\right), & j > 1, \text{even}, \\ \sqrt{\dfrac{2}{\Lambda}} \sin\left(\dfrac{2j\pi x}{\Lambda}\right), & j > 1, \text{odd}. \end{cases} \tag{6}$$

By Karhunen-Loéve expression, the stochastic process $h = h(\omega; x)$ can be expressed as

$$\begin{aligned} f(\omega; x) &= \sum_{j=0}^{\infty} \sqrt{\lambda_j} \xi_j \varphi_j \\ &= \sqrt{\lambda_0} \xi_0(\omega) \sqrt{\frac{1}{\Lambda}} \\ &+ \sum_{j=1}^{\infty} \sqrt{\lambda_j} \left[\xi_{j,s}(\omega) \sqrt{\frac{2}{\Lambda}} \sin\left(\frac{2j\pi x}{\Lambda}\right) + \xi_{j,c}(\omega) \sqrt{\frac{2}{\Lambda}} \cos\left(\frac{2j\pi x}{\Lambda}\right) \right]. \end{aligned}$$

Here ξ_0, and $\xi_{j,c}$, $\xi_{j,s}$, $j = 1, 2, \cdots$, are Gaussian random variable with the mean values of 0 and the variance of 1 and they are independent and identically distributed.

Alternatively, by letting

$$\lambda_j = \sigma^2 \bar{\lambda}_j \quad \text{where } \bar{\lambda}_j = \frac{\Lambda \hat{c}_j}{2},$$

we may express the profile of the random surface by

$$f(\omega; x) = \sigma \cdot \bar{f}(\omega; x), \tag{7}$$

where

$$\begin{aligned} \bar{f}(\omega; x) &= \sqrt{\bar{\lambda}_0} \xi_0(\omega) \sqrt{\frac{1}{\Lambda}} \\ &+ \sum_{j=1}^{\infty} \sqrt{\bar{\lambda}_j} \left[\xi_{j,s}(\omega) \sqrt{\frac{2}{\Lambda}} \sin\left(\frac{2j\pi x}{\Lambda}\right) + \xi_{j,c}(\omega) \sqrt{\frac{2}{\Lambda}} \cos\left(\frac{2j\pi x}{\Lambda}\right) \right]. \end{aligned} \tag{8}$$

It is clear that $\bar{h}$ is independent of the RMS height σ.

In practical computations, we can truncate the finite terms of Karhunen–Loève expansion. Since the covariance function $c(x)$ is smooth, its Fourier coefficients $\widehat{c}_0,\widehat{c}_1,\widehat{c}_2\cdots$ decays exponentially. Enough finite terms of Karhunen–Loève expansion ensures the accuracy of our algorithm.

3. Optimal design of random rough surface

3.1. Optimal design problem. For any sample $\omega \in \Omega$, according to the law of conservation of the energy,

$$R(\omega) + A(\omega) = 1.$$

Here $R(\omega)$ represents the reflectivity of the TCO layer and $A(\omega)$ represents the absorptivity of the absorption layer. The main purpose of the optimization design is to pursue the maximum value of the mean absorptivity $E(A(\omega))$, in other words, to find the minimum value of reflectivity mean $E(R(\omega))$. For each sample $\omega \in \Omega$, the reflectivity can be defined as,

$$R(\omega; h) = \sum_{n\in N} \frac{\eta_n}{\eta_0}|r_n(\omega)|^2,$$

where $N := \{n \in N | k_0^2\varepsilon_{r,2} - \alpha_n^2 > 0\}$ is the index of propagating modes,

$$r_n(\omega) = \begin{cases} \hat{u}_n(\omega; b)e^{-i\eta_n b}, & n \neq 0 \\ \hat{u}_n(\omega; b)e^{-ikb} - e^{-2ikb}, & n = 0, \end{cases} \tag{9}$$

which is inspired by

$$u^s(\omega; \cdot) =: \sum_{n=-\infty}^{\infty} r_n(\omega)e^{-i\alpha_n x + i\eta_n y}$$

$$r_n = \widehat{u}_n^s(\omega; b)e^{-i\eta_n b},$$

where $\widehat{u}_n^s$ is the Fourier coefficient of the scatter wave u^s. The expectation of reflectivity is

$$E[R] := \int_\Omega \sum_{n\in N} \frac{\eta_n}{\eta_0}|r_n(\omega)|^2 dP(\omega).$$

We define the cost function

$$J(\kappa) := E(R(\omega, h)),$$

where $\kappa := (\sigma, l)$ is a vector consists of the root mean square σ and the correlation l of $h(\omega, x)$.
The optimal design problem is to minimize J.

3.2. Shape derivative and the gradient of the cost function. We will apply the stochastic gradient descent method to find the minimum of $J(\kappa)$. First, we need to find the gradient of R.

Theorem 3.1. For each sample ω, the gradient $\nabla_\kappa R$ can be expressed as

$$\nabla_\kappa R = \frac{2}{\Lambda} \sum_{n\in N} \frac{\eta_n}{\eta_0} \mathrm{Re}[(\widehat{u}_n(\omega; b) - a_n e^{-ikb})\overline{(\varepsilon_{r,1}^{-1} - \varepsilon_{r,2}^{-1})} \cdot \int_0^\Lambda [W(x, h(x)) \cdot \nabla_\kappa h dx] \tag{10}$$

where

$$W(x,h(x)) := \begin{cases} \lim\limits_{\substack{(x,y)\to(x,h(x)),\\ (x,y)\in D_2}} \nabla u(x,y)\bar{u_n^*}(x,y),\ \nabla_\kappa h \text{ point to } D_2, \\ \lim\limits_{\substack{(x,y)\to(x,h(x)),\\ (x,y)\in D_1}} \nabla u(x,y)\bar{u_n^*}(x,y),\ \nabla_\kappa h \text{ point to } D_1, \end{cases} \tag{11}$$

$a_0 = 1$ and $a_n = 0 (n \neq 0)$, u is the solution of the scattering problem (5), and u_n^* is the solution of the following adjoint problem.

$$\begin{cases} \nabla(\varepsilon_r^{-1}\nabla u_n^*(\omega;\cdot) + k_0^2 u_n^*(\omega;\cdot) = 0 & \text{in } D\backslash\Gamma(\omega), \\ u_n^*(\omega;0,y) = u_n^*(\omega;\Lambda,y), & 0 < x_2 < b, \\ \partial_\nu u_n^*(\omega;x,0) = 0, & 0 < x < \Lambda, \\ \dfrac{\partial u_n^*}{\partial y}(\omega;x,b) = T^*(u_n^*(\omega;x,b)) + e^{i\alpha_n x} & 0 < x < \Lambda, \\ (u_n^*)_+(\omega;x,h(\omega,x)) = (u_n^*)_-(\omega;x,h(\omega,x)) & 0 < x < \Lambda, \\ \varepsilon_{r,2}^{-1}(\partial_\nu u_n^*)_+(\omega;x,h(\omega,x)) = \varepsilon_{r,1}^{-1}(\partial_\nu u_n^*)_-(\omega;x,h(\omega,x)) & 0 < x < \Lambda, \end{cases} \tag{12}$$

where T^* is the adjoint operator of T,

$$\langle Tu, v\rangle = \langle u, T^* v\rangle.$$

Proof: Denote $H^1(D) = \{u(x,y) | (\int_D |f(x)|^2 dx)^{\frac{1}{2}} < \infty,\ (\int_D |f'(x)|^2 dx)^{\frac{1}{2}} < \infty$ and $u(0,y) = u(\Lambda,y)\}$. The variational formula for (5) is $a(u,v) := \langle g, v\rangle,\ \forall v \in H^1(D)$, where

$$a(u,v) = \int_D \varepsilon_r^{-1}\nabla u \cdot \nabla\bar{v} - k_0^2 u\bar{v} d\mathbf{x} - \langle Tu, v\rangle. \tag{13}$$

Similarly, the variational formulation for (12) is denoted as $a^*(u_n^*, v) := \langle e^{i\alpha_n x}, v\rangle$, $\forall v \in H^1(D)$, where

$$a^*(u_n^*, v) = \int_D \varepsilon_r^{-1}\nabla u_n^* \cdot \nabla\bar{v} - k_0^2 u\bar{v} d\mathbf{x} - \langle T^* u_n^*, v\rangle. \tag{14}$$

With regard to the shape derivative $\nabla_\kappa R$, we know that the change of the reflectivity δR is caused by the change δh of the random surface h. If the interface $\Gamma = (x, h(x))$ is perturbed to be $\Gamma^\delta = (x, h^\delta(x))$. For the perturbed interface $\Gamma^\delta = (x, h^\delta(x))$, denote the total field as u^δ and the relative permittivity as ε_r^δ. The corresponding variation problem is $a^\delta(u^\delta, v) := \langle g, v\rangle,\ \forall v \in H^1(D)$, where

$$a^\delta(u,v) = \int_D (\varepsilon_r^\delta)^{-1}\nabla u^\delta \cdot \nabla\bar{v} - k_0^2 u^\delta\bar{v} d\mathbf{x} - \langle Tu^\delta, v\rangle. \tag{15}$$

Let $\delta u = u^\delta - u$ and $(\delta\varepsilon_r)^{-1} = (\varepsilon_r^\delta)^{-1} - \varepsilon_r^{-1}$, form (13) and (15) we have

$$\int_D \varepsilon_r^{-1}\nabla\delta u \cdot \nabla\bar{v} - k_0^2\delta u\bar{v} d\mathbf{x} - \langle T\delta u, v\rangle = -\int_D (\delta\varepsilon_r)^{-1}\nabla u^\delta\nabla\bar{v} d\mathbf{x} \tag{16}$$

Setting $v = \delta u$ in (14) and $v = u_n^*$ in (16) leads to

$$\begin{cases} \int_D \varepsilon_r^{-1}\nabla u_n^*\nabla\overline{\delta u} - k_0^2 u_n^*\delta u d\mathbf{x} - \langle T^* u_n^*, \delta u\rangle = \langle e^{i\alpha_n x}, \delta u\rangle \\ \int_D \varepsilon_r^{-1}\nabla\delta u\nabla\overline{u_n^*} - k_0^2\delta u\overline{u_n^*} d\mathbf{x} - \langle T\delta u, u_n^*\rangle = -\int_D (\delta\varepsilon_r)^{-1}\nabla u^\delta\nabla\overline{u_n^*} d\mathbf{x} \end{cases} \tag{17}$$

Therefore, we have

$$\langle e^{i\alpha_n x}, \delta u\rangle = -\int_D \overline{(\delta\varepsilon_r)^{-1}\nabla u^\delta\nabla u_n^*} d\mathbf{x} \tag{18}$$

$$= -\int_D \overline{(\delta\varepsilon_r)^{-1}\nabla u\nabla\overline{u_n^*}} d\mathbf{x} + O(\|(\delta\varepsilon_r)^{-1}\| \cdot \|\delta u\|) \tag{19}$$

For any test function $v \in H^1(D)$, there is an inner product,

$$(v, (\delta\varepsilon_r)^{-1}) := \int_D v(x)\overline{(\delta\varepsilon_r(x))^{-1}} = \int_{\mathrm{symdiff}(D_1, D_1^\delta)} v(x)\overline{(\delta\varepsilon_r(x))^{-1}}dx \tag{20}$$

Here D_1 and D_1^δ are the absorbing layers corresponding to the interface h and h^δ, respectively, and the symmetric difference between the two regions can be expressed as,

$$\mathrm{symdiff}(D_1, D_1^\delta) = (D_1 \cup D_1^\delta) \setminus (D_1 \cap D_1^\delta).$$

It is known that the relative permittivity value of the absorption layer and the TCO layer are $\varepsilon_{r,1}$ and $\varepsilon_{r,2}$,respectively. For an infinitesimal interface disturbance δh, the inner product can be simplified to

$$(v, (\delta\varepsilon_r)^{-1}) = \int_0^\Lambda v(x, h(x))\overline{(\varepsilon_{r,1}^{-1} - \varepsilon_{r,2}^{-1})}\delta h dx \tag{21}$$

For the new interface h^δ, the reflectivity at the sample ω is

$$\begin{aligned} R^\delta(\omega, h) &= \sum_{n\in\mathcal{N}} \frac{\eta_n}{\eta_0}\|r_n + \delta r_n\|^2 \\ &= \sum_{n\in\mathcal{N}} \frac{\eta_n}{\eta_0}\Big\{\|r_n\|^2 + 2Re[r_n\overline{\delta r_n}] + \|\delta r_n\|^2\Big\} \\ &= R(\omega, h) + 2\sum_{n\in\mathcal{N}} \frac{\eta_n}{\eta_0} Re[r_n\overline{\delta r_n}] + O(\delta h^2). \end{aligned}$$

We can get the influence of the disturbance $\delta R := R^\delta - R$ of the random surface h on the scattering rate is,

$$\delta R = 2\sum_{n\in N} \frac{\eta_n}{\eta_0} Re[r_n\overline{\delta r_n}] + o(\delta h^2)$$

With regard to the item $r_n\overline{\delta r_n}$ can be expressed as,

$$r_n\overline{\delta r_n} = \begin{cases} \hat{u}_n(\omega; b) \cdot \dfrac{1}{\Lambda}\displaystyle\int_0^\Lambda e^{i\alpha_n x}\ \overline{\delta u(\omega; x, b)}\ dx, & n \neq 0 \\ \big(\hat{u}_n(\omega; b) - e^{-ikb}\big) \cdot \dfrac{1}{\Lambda}\displaystyle\int_0^\Lambda e^{i\alpha_n x}\ \overline{\delta u(\omega; x, b)}\ dx, & n = 0. \end{cases}$$

Since

$$\int_0^\Lambda e^{i\alpha_n x}\ \overline{\delta u(\omega; x, b)} = -\int_D \overline{(\delta\varepsilon_r)^{-1}\nabla u\nabla\overline{u_n^*}}d\mathbf{x} + O(\|(\delta\varepsilon_r)^{-1}\| \cdot \|\delta u\|)$$

Substitute formula (21), it can be obtained by calculation,(18)

$$r_n\overline{\delta r_n} = \begin{cases} \widehat{u}_n(\omega; b) \cdot \frac{1}{\Lambda}\overline{(\varepsilon_{r,1}^{-1} - \varepsilon_{r,2}^{-1})} \cdot \int_0^\Lambda [W(x, h(x)) \cdot \delta h dx] \\ \qquad +O(\|(\delta\varepsilon_r)^{-1}\| \cdot \|\delta u\|) n \neq 0; \\ (\widehat{u}_n(\omega; b) - e^{-ikb}) \cdot \frac{1}{\Lambda}\overline{(\varepsilon_{r,1}^{-1} - \varepsilon_{r,2}^{-1})} \cdot \int_0^\Lambda [W(x, h(x)) \cdot \delta h dx] \\ \qquad +O(\|(\delta\varepsilon_r)^{-1}\| \cdot \|\delta u\|), n = 0. \end{cases}$$

where

$$W(x, h(x)) := \begin{cases} \lim\limits_{(x,y)\to(x,h(x))} \nabla u(x, y)\bar{u}_n^*(x, y), & \delta h > 0 \\ \lim\limits_{(x,y)\to(x,h(x))} \nabla u(x, y)\bar{u}_n^*(x, y), & \delta h < 0 \end{cases} \tag{22}$$

Finally, the disturbance of the scattering rate can be expressed as

$$\delta R = \frac{2}{\Lambda}\sum \frac{\eta_n}{\eta_0} Re[(\widehat{u_n}(\omega;b) - a_n e^{-ikb}) \cdot \overline{(\varepsilon_{r,1}^{-1} - \varepsilon_{r,2}^{-1})} \cdot \int_0^\Lambda [W(x,h(x)) \cdot \delta h dx] + O(\|(\delta\varepsilon_r)^{-1}\| \cdot \|\delta u\|)],$$

By chain rule, we have

$$\nabla_\kappa R = \frac{2}{\Lambda}\sum_{n\in N} \frac{\eta_n}{\eta_0} \mathrm{Re}[(\widehat{u}_n(\omega;b) - a_n e^{-ikb})\overline{(\varepsilon_{r,1}^{-1} - \varepsilon_{r,2}^{-1})} \cdot \int_0^\Lambda [W(x,h(x)) \cdot \nabla_\kappa h dx].$$

The proof is complete.

Note that both ε_r and $\nabla u \nabla u_n^*$ attain jumps across the interface Γ_ω. $\nabla_\kappa h$ is the gradient of h with respect to κ. The expression of the gradient of the mean reflectivity function is,

$$\nabla_\kappa J = \int_\Omega \nabla_\kappa R(\omega;h) dP(\omega).$$

3.3. Stochastic gradient descent method. With the gradient of J computed, we can apply gradient based iterative methods to find the minimizer of J. One of the most commonly used gradient method is the simple gradient descent (GD) method: given an initial guess κ_0 for κ,

$$\kappa_{k+1} = \kappa_k - \alpha_k \nabla_\kappa J(\kappa_k), \quad k = 0, 1, \cdots, \tag{23}$$

where α_k is the step size of each iteration. In practice, one needs to use the Monte Carlo method to approximate the expectation in $\nabla_\kappa J$: with independently drawn samples $\omega_1, \cdots, \omega_M$, $\nabla_\kappa J(\kappa) \approx \frac{1}{M}\sum_{i=1}^{M} \nabla_\kappa R(\kappa, \omega_i)$. Then (23) becomes

$$\kappa_{k+1} = \kappa_k - \alpha_k \frac{1}{M}\sum_{i=1}^{M} \nabla_\kappa R(\kappa_k, \omega_i), \quad , k = 0, 1, \cdots. \tag{24}$$

When M is very large, which is the case when the mesh size of the discretization for the Helmholtz equation is small, (24) is impractical because one must solve thousands of Helmholtz equations and their adjoints at each iteration. In this work, we adopt the stochastic gradient descent (SGD) method, which is commonly used in machine learning simulations. In the SGD method, we still need a sequence of independent samples $\omega_1, \omega_2, \cdots$. However, we only use one sample at each iteration:

$$\kappa_{k+1} = \kappa_k - \alpha_k \nabla_\kappa R(\kappa_k, \omega_k), \quad k = 0, 1, \cdots. \tag{25}$$

The numerical experiments in the following section shall demonstrate that the SGD iteration is far more efficient than the GD iteration.

4. Numerical experiments

In this part, we use two examples to show the effectiveness of the SGD algorithm in solving the proposed optimal design problems. The first numerical example serves as a verification of the accuracy of the numerical simulation of U. In the second example, the convergence of the optimization algorithm is tested. The absorbance of the obtained optimal random texture solar cells was compared with the flat surface.

In both examples, we set that the height of the reference plane is the same as the thickness of the absorption layer, assuming $a = 300nm$, the periodic size of battery $\Lambda = 1500nm$, in the ordinary gradient descent method, we choose the number of the Monte Carlo sampling $M = 1000$, the derivative $\nabla_\alpha R(\omega)$ is calculated by parallel

operation for different samples. We also demonstrate the result of the stochastic gradient method, which greatly saves the cost of numerical cost.

Example 1

The aim of this example is to verify the accuracy of the numerical solver for solving scattering problems. We assume that the wavelength $\Lambda_0 = 500nm$ in the free space has a refractive index of $q_1 = 2.0$ and $q_2 = 1.2$ in regions D_1 and D_2, respectively. We also assume that the interface is flat. Under the assumption that the incident wave is time-harmonic plane wave $u^i = e^{-ik_0q_2y}$, where k_0 is the wavenumber in free space, the analytical solution of the scattering problem u can be obtained in the following way.

$$u(x) = \begin{cases} e^{-ik_0q_2y} + c_2e^{ik_0q_2y}, \\ c_1(e^{ik_0q_1y} + e^{-ik_0q_1y}). \end{cases}$$

Thus

$$\nabla u(x) = \begin{cases} -ik_0q_2e^{-ik_0q_2y} + ik_0q_2c_2e^{ik_0q_2x_2}, \\ c_1(ik_0q_1e^{ik_0q_1y} - ik_0q_1e^{-ik_0q_1y}). \end{cases}$$

TABLE 1. L^2-norm of the error for the numerical solution at various mesh size and the corresponding convergence order.

Δ	12 nm	6 nm	3 nm	1.5 nm
$\|\|\tilde{u} - u_\Delta\|\|_{L^2}$	0.23134	0.0428	0.0136	0.00294
convergence order		2.01	2.03	1.98

Apply the continuity of the electric field and magnetic field, we have

$$e^{-ik_0q_2y} + c_2e^{ik_0q_2y} = c_1(e^{ik_0q_1y} + e^{-ik_0q_1y}),$$

$$q_1^2(-ik_0q_2e^{-ik_0q_2y} + ik_0q_2c_2e^{ik_0q_2y}) = q_2^2c_1(ik_0q_1e^{ik_0q_1y} - ik_0q_1e^{-ik_0q_1y}).$$

By direction calculation,

$$c_2 = \frac{c_1(e^{ik_0q_1a} + e^{-ik_0q_1a})}{e^{ik_0q_2a} - e^{-2ik_0q_2a}},$$

$$c_2 = \frac{c_1q_2(e^{ik_0q_1a} - e^{-ik_0q_1a})}{q_1e^{ik_0q_2a} + e^{-2ik_0q_2a}}.$$

Therefore, we can get

$$c_1 = \frac{2q_1e^{-ik_0q_2a}}{q_1(e^{ik_0q_1a} + e^{-ik_0q_1a}) - q_2(e^{ik_0q_1a} - e^{-ik_0q_1a})}.$$

Next we apply the element method with piecewise linear finite element spaces to solve the scattering problem. To this end, we set the mesh size $\Delta = 12nm, 6nm, 3nm, 1.5nm$. The corresponding $L^2 - norm$ form numerical error is listed in Table 1. From the table, we can see that the convergence order of the numerical method is about 2, which is consistent with the theoretical convergence order of the finite element method.

Next, we consider the random surface at a sample point with the root mean square (RMS) height $\sigma = 30nm$ and the correlation length $l = 24nm$. The regions are triangulated according to the mesh size $\Delta = 12nm, 6nm, 3nm, 1.5nm$. To test the convergence of the numerical solution of the partial differential equation, we choose the numerical solution u of the mesh size $\Delta = 0.6nm$ as the reference

TABLE 2. $||\tilde{u} - u_\Delta||_{L^\infty}$ for various mesh sizes along the boundary $x_2 = b$, where $\tilde{u}$ is the reference solution obtained with $\Delta = 0.06nm$.

Δ	12 nm	6 nm	3 nm	1.5 nm
$||\tilde{u} - u_\Delta||_{L^\infty}$	0.2918	0.0692	0.0125	0.0049

solution, and calculate the $L^\infty - norm$ error $\|u - u_\Delta\|_L^\infty$ of the numerical solution for the above four different triangulations. We can see clearly the convergence of the finite element method. In order to illustrate the scattering effect of rough surfaces, we also draw the total field of the scattering problem (Figure 4 and Figure 5) for mesh size $\Delta = 3$

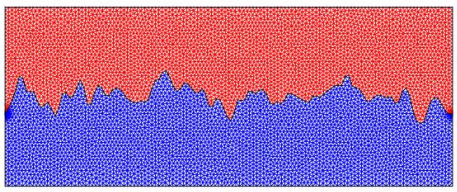

FIGURE 3. A mesh for a chosen sample.

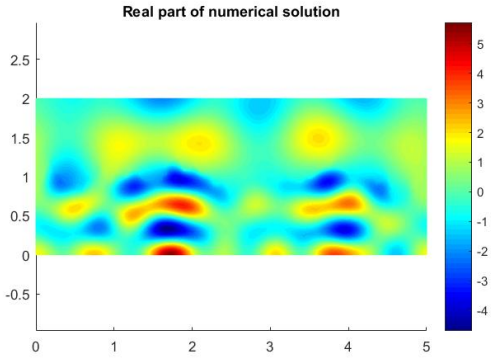

FIGURE 4. Real part of the total field with $\Delta = 3nm$.

TABLE 3. The value of σ and l for all iterations.

Iteration	0	1	2	3	...	10	11	12	13	14
σ	21	24.04	27.29	30.57	...	48.70	49.73	49.74	50.57	51.24
l	36	36.03	36.02	35.87	...	35.56	35.43	35.43	35.74	35.85

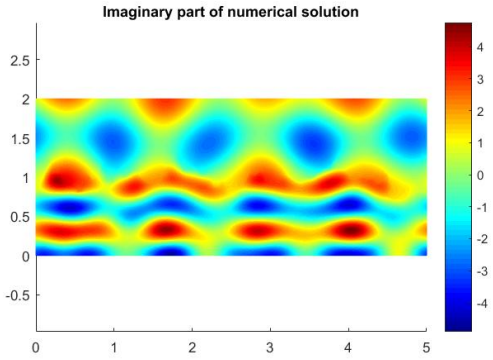

FIGURE 5. Imaginary part of the total field with $\Delta = 3nm$.

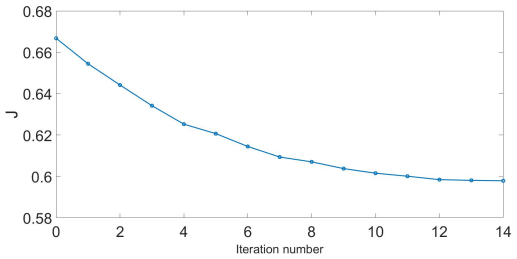

FIGURE 6. The cost function $J(\alpha)$ for all iterations.

Example 2

In this example, we assume that the wavelength in the vacuum is $\Lambda_0 = 650nm$, the refractive index of TCO layer is 1.915, or its relative permittivity $\varepsilon_{r1} = 3.667$, and the refractive index of the absorbing layer is $4.2 + 0.045i$ when $\Lambda_0 = 650nm$. This means that the relative index value of the absorbing layer is $\varepsilon_{r,2} = 17.6380 + 0.3780i$. In Figure 6 we depict the iteration diagram of the objective function $J(\kappa)$ using the gradient descent method with stepsize α_k chosen as $\frac{1}{k}$ and Monte Carlo sample size chosen as $M = 1000$. The iterative values of (σ, l) is given in Table 3.

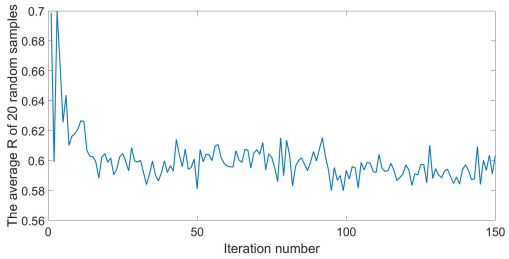

FIGURE 7. The cost function J for all iterations with stochastic gradient method.

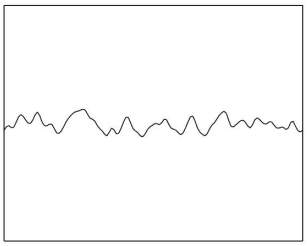

FIGURE 8. One random sample at initial parameter.

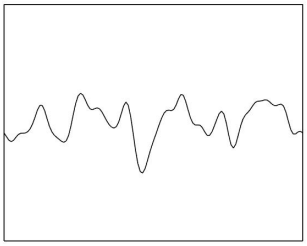

FIGURE 9. One random sample at optimal parameter.

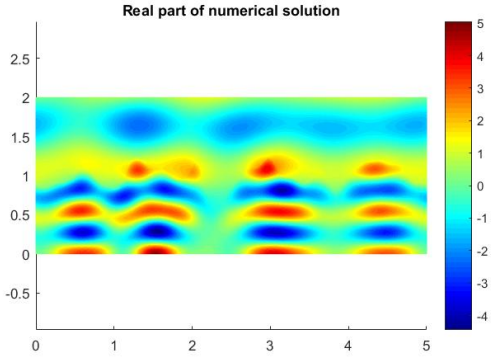

FIGURE 10. Real part of the total field of one sample after optimal design.

In Figure 7, we show the iteration diagram of J using the stochastic gradient descent method. We note that for the stochastic gradient descent method, only 300 numerical solutions for u and u_n^* are required for 150 iterations, whereas, for the gradient descent method, it requires 15000 solves for u and u_n^* It is obvious that the stochastic gradient method is far more efficient than the gradient descent method.

In Figure 8, we show a sample realization for the initial parameter, while in Figure 9 we show the realization of the random surface under the optimal statistical parameters. Figure 10 and Figure 11 depict the total field at optimal parameter κ at one sample.

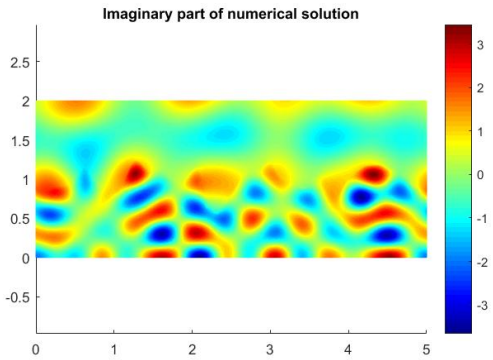

FIGURE 11. Imaginary part of the total field of one sample after optimal design.

TABLE 4. The absorptances of solar cells with different types of surfaces.

	flat surface	optimal surface
σ(nm)	0	51.24
l(nm)		35.85
E[A]	0.231	0.402

To demonstrate the optimal interface's efficiency in absorbing the solar energy, we calculate the absorptivity of solar cells with flat surface and the optimal random surface. It turns out that the absorptivity with a flat surface is 0.231. On the other hand, when the optimal random surface texture is used, the average absorptivity of solar cells is about 0.402, which is 74% increase over the flat surface.

References

[1] G. Beaucarne, Silicon thin-film solar cells, Adv. OptoElectronics, (2007), 10.1155/2007/36970.
[2] G. Bao, D. Dobson, and J. Cox, Mathematical studies in rigorous grating theory, J. Opt. Soc. Amer. A, 12 (1995), 1029-1042.
[3] G. Bao and Y. Wang, Optimal design of antireflection coatings with different metrics, J. Opt. Soc. Am. A, 30 (2013), 656-662.
[4] A. Bonnet-Bendhia and F. Starling, Guided waves by electromagnetic gratings and non-uniqueness examples for the diffraction problem, Math. Meth. Appl. Sci., 17 (1994), 305-338.
[5] C. Battaglia, et al. Light trapping in solar cells: can periodic beat random?, ACS Nano, 6 (2013): 2790-2797.
[6] J. Sokolowski and J. P. Zolesio, Introduction to Shape Optimization, Springer Berlin Heidelberg, 1992.
[7] M. Zeman, R. A. C. M. M. van Swaaij, and J. W. Metselaar, Optical modeling of a-Si:H solar cells with rough interfaces: Effect of back contact and interface roughness, J. Appl. Phys., 88 (2000), 6436-6443.
[8] G. Bao, Y. Cao, J. Lin, and H. W. Van Wyk Computational Optimal Design of Random Rough Surfaces in Thin-Film Solar Cells, Commun. Comput. Phys., 25 (2019), 1591-1612
[9] V. Ferry, et al. Optimized spatial correlations for broadband light trapping nanopatterns in high efficiency ultrathin film a-Si: H solar cells, Nano Lett., 11 (2011), 4239-4245.
[10] J. C. Goldschmidt *et al*, Increasing the efficiency of fluorescent concentrator systems, Sol. Energy Mat. Sol. Cells, 93 (2009), 176-182.

[11] P. Kowalczewski, M. Liscidini, and L. Andreani, Engineering Gaussian disorder at rough interfaces for light trapping in thin-film solar cells, Opt. Lett., 37 (2012), 4868-4870.
[12] S. Nicolay, M. Despeisse, F.-J. Haug, and C.Ballif, Control of LPCVD ZnO growth modes for improved light trapping in thin film silicon solar cells Solar Energy Materials and Solar Cells, 95 (2011), 1031-1034.
[13] L. Bottou, O. Bousquet, Optimization for Machine Learning, Cambridge: MIT Press, 2012.
[14] R.G. Ghanem, P.D. Spanos, Stochastic Finite Elements: a Spectral Approach, Springer-Verlag, 1991.

1 College of Intelligent Systems Science and Engineering, Harbin Engineering University, Harbin, Heilongjiang, 150001,China.
E-mail: wangdancat@hrbeu.edu.cn

2 Department of Mathematics and Statistics, Auburn University, Auburn, AL, 36849, USA.
E-mail: yzc0009@auburn.edu

3 Department of Mathematics and Statistics, Auburn University, Auburn, AL, 36849, USA.
E-mail: qzl0011@auburn.edu

4 College of Intelligent Systems Science and Engineering, Harbin Engineering University , Harbin, Heilongjiang, 150001,China,
E-mail: shenjihong@hrbeu.edu.cn corresponding author